TAMPEREEN TEKNILLINEN YLIOPISTO
TAMPERE UNIVERSITY OF TECHNOLOGY
Julkaisu 583 • Publication 583

Luís Gomes

Ultrafast Ytterbium Fiber Sources Based on SESAM Technology

Tampere 2006

Tampereen teknillinen yliopisto. Julkaisu 583
Tampere University of Technology. Publication 583

Luís Gomes

Ultrafast Ytterbium Fiber Sources Based on SESAM Technology

Thesis for the degree of Doctor of Technology to be presented with due permission for public examination and criticism in Tietotalo Building, Auditorium TB104, at Tampere University of Technology, on the 27th of January 2006, at 12 noon.

Tampereen teknillinen yliopisto - Tampere University of Technology
Tampere 2006

ISBN 952-15-1521-X (printed)
ISBN 952-15-1801-4 (PDF)
ISSN 1459-2045

Abstract

In this thesis we report on the experimental studies on the generation of ultrashort pulses from mode-locked ytterbium fiber lasers operating at 1 μm wavelength region. Different fiber cavities, all with a linear geometry, were studied. The passive mode-locking investigated here was based on SESAM technology. GaInAs and GaInNAs material systems were explored as saturable absorbers. The results obtained with the GaInNAs SESAMs demonstrated that these reflectors can be faster than the mirrors made of GaInAs. This allowed shorter optical pulses to be achieved from ytterbium fiber lasers with saturable absorbers based on dilute nitride, and suggests that using dilute nitride material system allows avoiding post-growth actions needed for reducing the absorption recovery time and, therefore, making SESAM technology more efficient and cost-effective.

The cavity configuration which was studied allowed for tunable pulse operation in three adjacent wavelength bands which cover the spectral range from 977 to 1115 nm. The typical pulse width was in the picosecond range with an average output power of tens of mW. The amplification of these pulses in a cladding-pumped fiber amplifier up to average power over 700 mW has been demonstrated, that corresponds to a peak power of 6 kW and a pulse energy of about 23 nJ. Using a grating pair for dispersion compensation inside the cavity, pulses as short as 1 ps were achieved. External pulse compression was also used resulted in 340 fs duration pulses.

The generation of mode-locked pulses in a cavity without dispersion compensation was also studied using a short-length cavity with a doped fiber placed inside a loop mirror. The self-starting mode-locked operation with overall normal cavity dispersion was initiated and stabilized with optimized high-performance SESAMs.

In another cavity using the dispersion compensation by a Gires–Tournois interferometer (GTI), the reduction of the pulse duration by an order of magnitude was achieved, as compared to the pulses obtained without dispersion compensation.
To conclude, the main result of this work is an extensive study of SESAM technology for mode-locking of fiber lasers in the 1 μm wavelength region. The results which should be emphasized are

– the demonstration of GaInNAs SESAMs in short-wavelength region (<1.1 μm),
– broadly tunable mode-locked ytterbium fiber oscillator,
– dispersion compensation free fiber lasers mode-locked with SESAMs,
– the use of a compact GTI for dispersion compensation in a fiber cavity.

Acknowledgements

This work was carried out at the Optoelectronics Research Centre (ORC) of the Tampere University of Technology (TUT). I gratefully acknowledge the financial support provided by the Portuguese Foundation for Science and Technology (FCT), and of the European Union's Marie Curie fellowship program.

My deepest gratitude goes to my supervisor, Professor Oleg Okhotnikov, for is invaluable support and guidance. Working with him has been a remarkable experience, following his high standard of scientific work. His unrelenting commitment to research is something I will always remember. I would also like to thank Professor Markus Pessa, the Director of the ORC, for the encouragement and support I always received from him. I'm also grateful for my supervisor in the Faculty of Sciences of the University of Porto, Professor Manuel Joaquim Marques, for his support and responsibility he made me feel during my work.

But this, like any other work, was teamwork. And it would never have been possible without the contributions and support of the whole ORC team. I would specially like to thank all the colleagues in the Ultrafast and Intense Optics Group, especially Mircea Guina, Matei Rusu, Antti Härkönen, Antti Isomäki, Lasse Orsila, Markus Peltola and Robert Herda. Without their assistance and encouragement I could not have done the work presented here. But above all, I must thank them for making my stay in Finland an enjoyable and memorable experience. I would also like to thank Ning Xiang, Anne Vainiopää and Tomi Jouhti for providing me with the samples they painstakingly grew for our experiments. I would also like to thank Anne Viherkoski for all her assistance in sorting out the administrative issues.

I would also like to thank my friends in Portugal, who always supported me when I was feeling down, and that helped me keep in touch with my Home. Finally my warmest thank you goes to my family, especially my parents, for understanding and encouraging all my decisions, and for the love and freedom they always give me.

Contents

List of Publications

[Paper I] “Mode-locked ytterbium fiber laser tunable in the 980–1070 nm spectral range”, O. G. Okhotnikov, **L. A. Gomes**, N. Xiang, T. Jouhti and A. Grudinin, Optics Letters, vol. 28, pp. 1522–1524, September 2003.

[Paper II] “980-nm picosecond fiber laser”, O. G. Okhotnikov, **L. A. Gomes**, N. Xiang, T. Jouhti, A. K. Chin, R. Singh and A. B. Grudinin, IEEE Photonic Technology Letters, vol. 15, p. 1519–1521, November 2003.

[Paper III] “Picosecond SESAM-based Ytterbium Mode-Locked Fiber Lasers”, **L. A. Gomes**, L. Orsila, T. Jouhti and O. G. Okhotnikov, Journal of Selected Topics on Quantum Electronics, vol. 10, pp. 1902–1906, January/February 2004.

[Paper IV] “Mode-locked ytterbium fiber lasers”, L. Orsila, **L. A. Gomes**, N. Xiang, T. Jouhti and O. G. Okhotnikov, Applied Optics, vol. 43, pp. 129–136, March 2004.

[Paper V] “Mode-locked ytterbium fiber laser tunable in the 980–1070 nm spectral range”, **L. A. Gomes**, N. Xiang, T. Jouhti, O. G. Okhotnikov and A. Grudinin, 87th OSA Annual Meeting “Frontiers in Optics”, Tucson, Arizona, USA, October 2003.

[Paper VI] “140-MHz stretched pulse ytterbium fiber laser operating in the 980–1030 nm spectral range”, **L. A. Gomes**, N. Xiang, T. Jouhti, O. G. Okhotnikov, M. Hotoleanu, A. Salomaa and S. Tammela, 87th OSA Annual Meeting “Frontiers in Optics”, Tucson, Arizona, USA, October 2003.

Author's Contributions

This thesis includes 6 papers published in open literature.

The work presented here is a result of the efforts of a whole team, without whom it would have been impossible to complete this task. Personally, I was directly responsible for designing, building and characterizing the fiber lasers and experimental setups presented in this thesis. The main focus was on the application of SESAM's to fiber lasers, with an aim to achieve mode locking in the 1 μm region of the optical spectrum. This task required an extensive development effort, especially as to the optimization of the different cavity configurations and SESAM properties. The task was performed in a close collaboration with my supervisor.

A list of my contributions to the research itself and preparing the scientific papers is given in the Table below.

Table. *Author's contribution to the papers and research work.*

Paper	Author's contribution in research work	Author's contribution in writing of the paper
Paper I	Group work (80%)	Co-author (50%)
Paper II	Group work (50%)	Main author
Paper III	Group work (50%)	Co-author (50%)
Paper IV	Group work (10%)	Co-author (10%)
Paper V	Group work (50%)	Main author
Paper VI	Group work (80%)	Main author

List of Abbreviations

A-FPSA	Antiresonant Fabry-Pérot Saturable Absorber
AR-SESAM	Anti-Reflection-coated SESAM
ASE	Amplified Spontaneous Emission
CFBG	Chirped Fibre Bragg Grating
CW	Continuous Wave
DBR	Distributed Bragg Reflector
D-SAM	Dispersive Saturable Absorber Mirror
GDD	Group Delay Dispersion
GVD	Group Velocity Dispersion
GTI	Gires–Tournois Interferometer
MBE	Molecular Beam Epitaxy
MOPA	Master Oscillator Power Amplifier
NLS	Nonlinear Schrödinger Equation
PBG	Photonic Band-Gap
PCF	Photonic Crystal Fibers
QW	Quantum Well
SBR	Saturable Bragg Reflector
SESAM	Semiconductor Saturable Absorber Mirror
SHG	Second Harmonic Generation
SPM	Self-Phase Modulation
TBP	Time-Bandwidth Product

1 Introduction

The remarkable progress in the telecommunications industry achieved in recent years has made an optical fiber technology a mature sector of the world industry. Consequently, the improvements in a fiber technology have resulted in significant development in related fields, for instance, the fiber lasers that intensively enter into the applications which previously were covered exclusively by solid-state lasers. In particularly, the area of tunable ultra-short optical pulse generation has been dominated so far by the Ti:Sapphire lasers.

With its broad-gain bandwidth, high optical conversion efficiency, and large saturation fluency an ytterbium doped fiber is a very promising medium for the generation and amplification of tunable short and ultrashort pulses around the 1 μm spectral range. Another interesting property of an Yb-doped fiber is that it can be made to work at 977 nm, thus opening the possibility to produce 488 nm radiation through second harmonic generation (SHG). Such a source could be an attractive alternative to bulky and inefficient Ar-lasers.

The main problem to be resolved when developing the mode-locked fiber lasers at short wavelength range (<1.3 μm) is the large value of normal dispersion of the fiber. Therefore, very few successful reports on short pulse fiber lasers in this region can be found, despite a continuous interest in compact fiber oscillators. The dispersion compensation in a cavity is usually achieved by using a grating pair or prism sequence. These devices make the cavity bulky, and the laser loses an elegant all-fiber form. A new solution that uses photonic bandgap (PBG) fibers is, as yet, on the early stage of development and its potential for dispersion compensation in fiber lasers is still to be carefully examined. Another well-known alternative is a Gires–Tournois interferometer (GTI). This approach, however, is generally not suitable for fiber lasers, because fiber cavities tend to exhibit dispersion larger than a GTI can compensate for.

It would be extremely desirable to ensure strong mode-locking mechanism that could initiate self-starting short pulse operation in a wide range of cavity dispersion. Since the demonstration of the first passively mode-locked laser, different saturable absorbers have been applied to initiate and maintain the pulse generation. In the 1990's, a new type of absorber was developed, a so-called semiconductor saturable absorber mirror (SESAM). Today, it is one of the most efficient triggers for pulse operation. SESAMs are used for mode-locking fiber lasers, solid-state lasers, disc laser and semiconductor lasers. An attractive feature of the SESAM technology is that the parameters of the reflector, e.g. the operation wavelength, saturation fluency and nonlinear response, could be conveniently adjusted.

In this thesis, we report on the experimental studies on mode-locked Yb-doped fiber lasers using various saturable reflectors and compensation schemes. Notably, we demonstrated a new GaInNAs-based SESAM for mode-locking fiber lasers at 1 μm. The broad wavelength tunability of such lasers was also demonstrated, along with the amplification of the pulses using a master oscillator power amplifier (MOPA) setup.

Another laser cavity examined in this thesis relies on a specially made gain fiber with a very high concentration of Yb-ions. With this fiber, the total length of the cavity could be reduced down to a few centimeters resulting, therefore, in an exceptionally low value of the overall cavity dispersion. With a short-length cavity, the use of a GTI for dispersion compensation has been successfully demonstrated, as well.

2 Theory

In this chapter the main theoretical aspects of the work are reviewed. The subjects to be considered are related to:

i) the properties of Yb-doped fiber amplifiers,
ii) dispersion properties of optical fibers and dispersion compensation techniques used in fiber lasers,
iii) the principles of passive mode-locking,
iv) a general description of semiconductor saturable absorber mirrors (SESAMs); their property and performance.

2.1 Properties of Yb-doped optical fibers

Since their development in the 1970's, optical fibers have become an essential component in many devices and systems [1]. They have found applications in imaging, sensing, telecommunications, material processing and many other fields of modern industry. The main advantage of the optical fibers, which are represented on Figure 2.1, is that they have low losses, and owing to the excellent beam confinement, the single mode regime can be easily achieved. The optical fibers have huge potential for high-capacity data transmission. All tools and instruments needed to handle the fiber are available commercially.

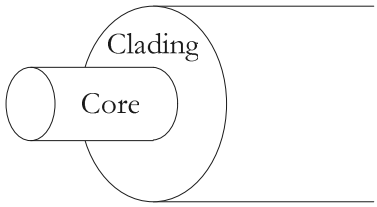

Figure 2.1 – Basic geometry of an optical fiber.

Optical fibers doped with rare-earth ions are almost ideal media for the generation and amplification of light, including radiation in the form of ultra-short optical pulses [2]. This property stems from the combination of the excellent light propagation characteristics of an optical fiber and the large absorption and emission cross sections of the active ions. Light amplification in rare-earth ion doped fibers has been exploited for the development of many important devices, such as fiber amplifiers used for optical telecommunications and a variety of fiber lasers.

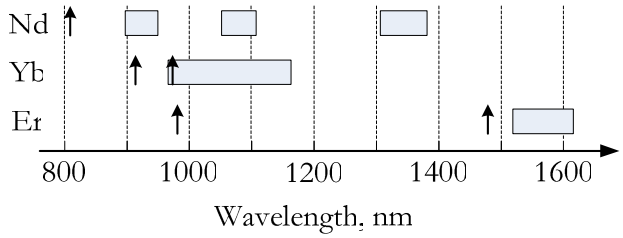

Figure 2.2 – Gain spectral bands of the fibers doped with different ions.

Figure 2.2 is a schematic representation of the gain spectral bands of the three most popular active rare-earth-doped fibers: Nd, Yb and Er. The arrows in the diagram indicate the wavelengths used to pump those ions, the rectangles represent the gain regions. As shown, the ideal ion for emission around 1 μm wavelength range is Yb, which exhibits a very broad gain bandwidth from 975 to over 1150 nm. Two spectral bands can be used for pumping the Yb-ions. One is ~915 nm and the other one is 980 nm. The spectra for the absorption and emission cross sections of Yb ions with silica as a host material are shown in Figure 2.3.

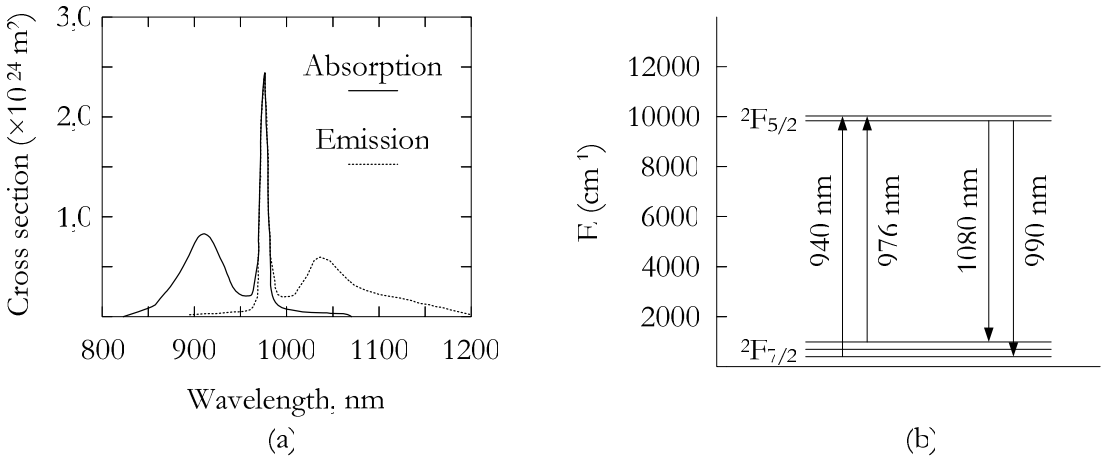

Figure 2.3 – (a) Absorption and emission cross sections and (b) energy diagram of Yb-doped fibers [3].

From the cross-section spectra of Figure 2.3 it is clear that pump light absorption at 980 nm is several times higher than absorption at 915 nm; the absorption bandwidth, however, is larger at 915 nm. This results in a very high pumping efficiency at 980 nm, but requires narrow-band spectrally stabilized pump source. Pumping at 915 nm, although less efficient, is attractive due to the very broad absorption bandwidth. Furthermore, pumping at 915 nm enables emission in the 980 nm region, which is important for frequency conversion.

The 980-nm fiber lasers have important applications in telecommunications and aerospace where they can be used to pump multiple erbium-doped fiber amplifiers. When frequency-doubled to 490 or 488 nm, they are replacement candidates for argon ion lasers for use in instrumentation in many analytical and bio-medical applications. For example, Southampton Photonics Inc. (SPI) and the Optoelectronics Research

Centre at the University of Southampton have reported 3.5 W of output power at 980 nm from a jacketed air-clad ytterbium-doped fiber laser [4].

2.2 Dispersion in optical fibers

Dispersion is a measure of the temporal broadening of optical pulses as they propagate in materials. Usually two different definitions are used, that may cause confusion. To avoid such confusion, the two definitions are presented here, along with the relationship between them [5]. The definition of the group velocity, V_g, of a mode propagating in a fiber with propagation constant β is

$$V_g = \left(\frac{d\beta}{d\omega}\right)^{-1} = c\left(\frac{d\beta}{dk}\right)^{-1}, \tag{2.1}$$

where ω is the angular frequency, k is the wave number and c is the speed of light. The group delay, τ_g, is given by

$$\tau_g = \frac{L}{V_g} = \frac{L}{c}\frac{d\beta}{dk} = -\frac{L\lambda^2}{2\pi c}\frac{d\beta}{d\lambda}, \tag{2.2}$$

where L is the length of the fiber and λ is the wavelength of the radiation. Assuming that the pulse has a spectral width $\Delta\omega$, the temporal (dispersion) broadening of the pulse, ΔT, is given by

$$\Delta T = \left|\frac{d\tau_g}{d\omega}\right|\Delta\omega = \frac{d}{d\omega}\left(\frac{L}{V_g}\right)\Delta\omega = L\frac{d^2\beta}{d\omega^2}d\omega = L\beta_2\Delta\omega, \tag{2.3}$$

where the Group Velocity Dispersion, GVD, is defined as

$$\beta_2 = \frac{d^2\beta}{d\omega^2}. \tag{2.4}$$

This parameter is usually expressed in [ps^2/km]. Another definition for dispersion is derived from expression (2.3) written in terms of the wavelength increment $\Delta\lambda$:

$$\Delta T = \left|\frac{d\tau_g}{d\lambda}\right|\Delta\lambda = \frac{d}{d\lambda}\left(\frac{L}{V_g}\right)\Delta\lambda = LD\Delta\lambda, \tag{2.5}$$

where D is the Group Delay Dispersion, GDD, defined as

$$D = \frac{d}{d\lambda}\frac{1}{V_g}. \tag{2.6}$$

This parameter is usually expressed in [ps/nm/km], and can be related to the GVD by the expression:

$$D = -\frac{2\pi c}{\lambda^2}\beta_2. \tag{2.7}$$

When the GVD is positive, the dispersion is said to be normal, and anomalous when the GVD is negative. If one uses GDD instead of GVD, the signs are obviously reversed. It should also be mentioned that expression (2.3) is valid only when $\Delta\omega$ is small, otherwise higher order terms must be considered:

$$\beta(\omega) = \beta(\omega_0) + \beta_1\Delta\omega + \frac{1}{2}\beta_2 \cdot \Delta\omega^2 + \frac{1}{6}\beta_3 \cdot \Delta\omega^3 + \frac{1}{24}\beta_4 \cdot \Delta\omega^4 + \ldots \,, \qquad (2.8)$$

where the higher-order terms in the expansion are defined as

$$\beta_n = \left.\frac{d^n\beta}{d\omega^n}\right|_{\omega=\omega_0} . \qquad (2.9)$$

The terms β_3 and β_4 are the third and fourth order dispersion terms. They should be taken into account when analyzing the propagation of ultra-short optical pulses with duration on a femtoseconds time scale. However, the study reported in this thesis, is mainly limited to picosecond-range pulses. Therefore, the higher order dispersion terms may be neglected and are not considered here.

In a simple arrangement of a laser cavity and a dielectric material therein, such as fiber gain medium, fiber passive components and SESAM, total cavity GDD for wavelengths shorter than 1 µm is usually positive. In other words, shorter wavelength light experiences a higher refractive index and a lower group velocity. This causes lengthening of a laser pulse per each round trip and prevents stable, short-pulse operation.

As shown in Figure 2.4, the dispersion in a single mode optical fiber has two main origins: the dispersion of the material and the dispersion of the waveguide. These two factors are not entirely independent, but usually they can be calculated separately, unless one needs an extremely rigorous calculation of the dispersion.

Material dispersion originates from the dependence of the refractive index with the wavelength of the radiation. A fraction of the mode propagates in the cladding of the fiber, which has different refractive index than the core of the fiber. The waveguide dispersion comes from the fact that the confinement factor which indicates the ratio of light propagating within the core to the total mode intensity, is wavelength-dependent.

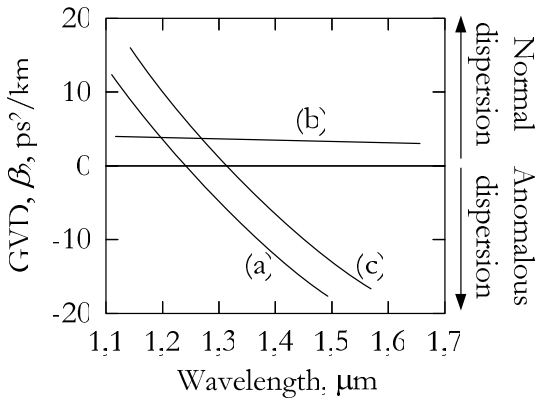

Figure 2.4 – Contributions of (a) material and (b) waveguide dispersion to (c) total dispersion [6].

The material dispersion is normal for short wavelengths (<1.2 μm), while the waveguide dispersion is normal at any wavelength (even for the fibers with different waveguide geometries, e.g. for so-called dispersion shifted or dispersion flattened fibers). As a result, the total dispersion in conventional index guided fibers is normal for wavelengths below 1.3 μm. When the fiber cavity is used to build an ultrashort pulse source, it is desirable to operate the laser at a low-value anomalous dispersion to reduce the pulse duration and to enhance the pulse shortening mechanism due to soliton formation [7]. Therefore, in order to support the ultrashort pulse length of an ultrafast laser, the laser must possess a total negative group-delay-dispersion, (negative GDD) i.e., the sum of the GDD of the laser gain medium and all the cavity components must be negative.

New types of optical fibers, such as PCF [8] or PBG fibers [9], can be designed to have anomalous dispersion in the 1-μm wavelength range or even at shorter wavelengths. However, the use of such fibers as intracavity elements in a fiber laser is a challenging solution because the optical structure of these fibers is very different from the structure of conventional index guided fibers. Therefore, alternative dispersion compensation techniques are considered in this study to enable the generation of short optical pulses.

2.2.1 Dispersion compensation with diffraction gratings

The use of a pair of diffraction gratings for dispersion compensation in a laser cavity is a well-known technique applied to solid state and fiber laser systems [10]. Figure 2.5 shows schematically a typical dispersion compensation setup comprising a grating pair and a mirror. Two pairs of gratings can also be used; this configuration allows for a system with ring cavity operating in traveling-wave regime.

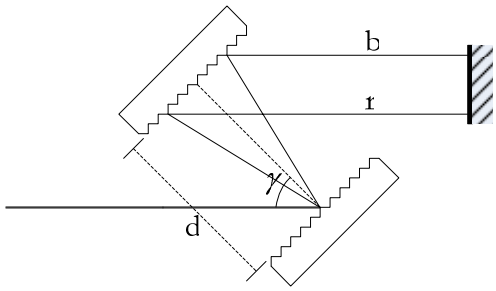

Figure 2.5 – Dispersion compensation with grating pairs.

The dispersion compensation effect in a grating pair arises from the fact that spectral components with shorter wavelengths (b – blue) travel a shorter distance than do spectral components with longer wavelengths (r – red). The difference in travel lengths is

$$\Delta L = d\frac{1+\cos\theta}{\cos(\gamma-\theta)}, \tag{2.10}$$

where d is the distance between the gratings, γ is the incidence angle. The angle θ is given by

$$\theta(\lambda) = \gamma - \arcsin\left(\frac{\lambda}{f} - \sin\gamma\right). \tag{2.11}$$

Here f is the separation between the fringes of the gratings. Finally, the GVD generated by this system is given by [10]

$$\beta_2 = \frac{d^2\beta}{d\omega^2} = -\frac{\lambda^3 d}{\pi c^2 f^2}\left[1-\left(\frac{\lambda}{f}-\sin\gamma\right)^2\right]^{-3/2}. \tag{2.12}$$

From Equation (2.12) it is clear that one can obtain large anomalous dispersion at any wavelength as long as the gratings with a proper spatial frequency and separation distance are used. However, the grating pairs have a disadvantage of being bulky free-space optical components, which introduce significant losses and increase the size and complexity of a fiber-based system.

2.2.2 Dispersion compensation with a Gires–Tournois Interferometer (GTI)

A GTI consists of a partially reflective top mirror, a cavity and a second mirror with a very high reflectivity [11]. Figure 2.6 shows a simplified scheme of a GTI, which is composed of a layer of refractive index n_1, and width e, and a bottom perfectly reflecting surface.

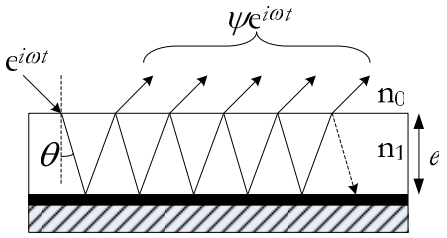

Figure 2.6 – Scheme of a Gires–Tournois Interferometer.

Its group-delay spectrum exhibits resonances that are characteristic of the transmission spectrum of Fabry-Perot interferometers. In 1964 Gires and Tournois [11] first suggested the use of these interferometers for pulse compression, and in 1969 the GTI compressor was used to achieve the mode-locked picosecond pulses from a He-Ne laser. Recently, Kuhl and Heppner used GTI for intracavity chirp compensation [12], [13].

It can be shown that delay time τ_g of light reflected from a GTI structure is

$$\tau_g = \frac{t_0\left(1-r^2\right)}{\left(1+r^2\right)-2r\cos\omega t_0} = t_0\frac{1+r}{1-r}\frac{1}{1+\frac{4r}{(1-r)^2}\sin^2\left(\frac{\omega t_0}{2}\right)}, \qquad (2.13)$$

where r is the reflectivity of the top mirror, and t_0 is the time it takes for the light to propagate once through the layer ($t_0 = 2en\cos\theta/c$). The dispersion of the GTI can now be estimated using the expression (2.3). Results of calculations for a device with a top reflectivity r = 0.9 and width e = 2.1 μm, assuming normal incidence and a refractive index n = 3, are shown in Figure 2.7.

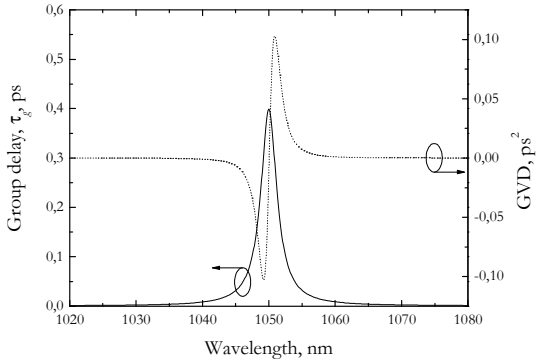

Figure 2.7 – Group delay (τ_g) and group velocity dispersion (GVD) generated by a GTI.

For a real device, with a bottom reflectivity slightly lower than “1”, the shape of these curves is not affected, although the generated dispersion is slightly smaller. More important effect is the appearance of a resonance dip in the reflectivity curve of the whole device. This dip limits the operation bandwidth of the device and it can introduce losses in the cavity thus limiting its applicability for intracavity dispersion compensation in a fiber laser. On the positive side, the GTIs can be integrated

together with semiconductor saturable absorber mirrors in a compact device that simplifies the architecture of a pulsed fiber laser [14].

The obvious disadvantage of the GTIs is that the GVD is strongly dependent upon the wavelength of the light incident thereon, as seen from Figure 2.7, which shows variation of the group velocity dispersion of a Gires–Tournois interferometer with respect to the wavelength of the incident light. This dependence is periodic in nature, the feature characteristic of multiple-beam interferometers like a Fabry-Pérot etalon. The variation in GVD with wavelength poses a significant practical problem when using a Gires–Tournois interferometer in a tunable pulsed laser. More specifically, in order to form highly stable soliton-like pulses, the group velocity dispersion must be accurately controlled and maintained. Unfortunately, as the wavelength of the laser is tuned, the GVD of the Gires–Tournois interferometer will vary. This effect will cause the pulse formation to become unstable to the point where the laser will no longer operate in the pulsed mode.

2.3 Operating regimes of a laser

The operating regimes of the laser can be classified on the basis of temporal characteristics of output emission. The most important regimes are continuous wave (CW), Q-switching, mode-locking, and Q-switched mode-locking [15]. They are depicted in Figure 2.8. In CW operation, the laser output is obviously stationary in time, while in the other regimes the output is time dependent.

A Q-switched laser is a device to which the technique of active or passive Q-switching is applied, so that it emits high-energy pulses [16]. In Q-switching technique, the cavity losses are kept on a high level until the gain medium has stored a significant amount of energy supplied by the pump source. Then, the losses are suddenly reduced down to a small value, so that the power of the laser radiation in the cavity builds up. This results in a pulse, the energy of which can be in the millijoule range even for rather small lasers. The decrease of optical loss corresponds to an increase in the Q-factor of the cavity. The cavity losses can be switched by applying different techniques. Active Q-switching uses a control element driven from an external electrical generator, e.g. an acousto-optic or electro-optic modulator. With this approach, the pulse is shaped shortly after an electrical signal arrives to the modulator. The achieved pulse energy and pulse duration depends on the energy stored in the gain medium. Passive Q-switching is performed by placing the saturable absorber in the laser cavity. The energy and duration of the Q-switched pulse is determined by the cavity and switching parameters, while the pulse repetition rate is determined by the pump power.

Q-switching allows for the generation of low repetition rates of high-energy pulses with durations much longer than those obtained with mode-locking. The pulse width in a Q-switching regime is typically in the nanosecond range (corresponding to several cavity round trips), and the pulse repetition rate ranges typically from 1 kHz to tens of kHz. The most common type of a Q-switched laser is the actively Q-switched one. The highest pulse energies and shortest pulse durations can be obtained with low repetition rates, however, at the expense of lower average output power.

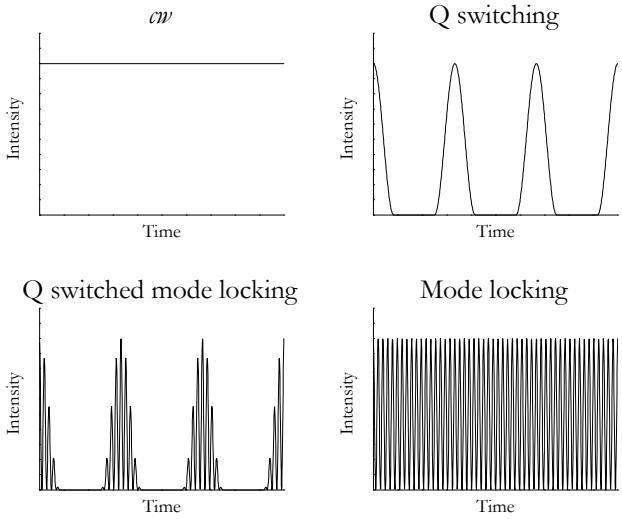

Figure 2.8 – Four main laser operation regimes.

Mode-locking is a method to obtain ultrashort pulses from a laser. When considered in the frequency domain, mode-locked laser generates a short pulse in the cavity, when a fixed phase relationship is achieved between its longitudinal modes. As in a Q-switched laser, either an optical modulator or a nonlinear component, such as saturable absorber, needs to be incorporated into the laser cavity to yield an ultrashort pulse circulating in the laser cavity [17]. The pulse repetition period corresponds to the round-trip time (typically 10–100 ns), while the pulse duration is typically between tens of fs and tens of ps.

Active mode-locking in a fiber laser is usually achieved with a Mach-Zehnder integrated-optic modulator, or with a semiconductor electroabsorption modulator that have a waveguide structure well-matched with an optical fiber. The period of the modulator signal should correspond to the round-trip time of the cavity. Higher repetition rate of the pulse trains can be obtained with harmonic mode-locking, which is the regime where multiple pulses are circulating in the laser cavity. The achieved pulse duration is typically in the picosecond range and is only weakly dependent on parameters like modulator signal strength. Passive mode-locking could provide much shorter pulses, because a saturable absorber with a short recovery time modulates the cavity losses much faster than any electronic modulator. Saturable absorbers for passive mode locking can be actual absorber devices, for example, semiconductors

using band-to-band absorption, or structures that induce an effective loss modulation using nonlinear effects. The popular form of a nonlinearity utilized in a solid-state laser is a Kerr lens mode-locking [18], while in fiber laser convenient method of Kerr nonlinearity is nonlinear polarization rotation in a fiber.

Although actively mode-locked lasers produce longer pulses as compared with passively mode-locked oscillators, an important advantage of this technique is that an output pulse train is synchronized to an external signal. This feature is particularly important for telecommunication applications requiring the locking of an optical signal to the clock. These sources representing optical clock generators are developed based on 1.55-μm erbium-doped mode-locked fiber lasers and are available commercially.

The pulse duration from passively mode-locked lasers is determined by the interplay of the characteristics of the saturable absorber and the parameters of the laser cavity, e.g. dispersion and gain dynamics. Passive mode-locking has been used with different fiber systems operating in a broad wavelength range, e.g. 900-nm, 980-nm, 1-μm and 1.55-μm [19–22].

Although passively mode-locked lasers usually produce shorter pulses than do actively driven systems, they may suffer from instabilities (amplitude fluctuation and timing jitter). Another harmful effect evolving in passively mode-locked systems is the fact that the saturable absorber reduces the damping of the relaxation oscillations. If this damping reduction effect is strong enough, then the relaxation oscillations become undamped and the pulse energy undergoes large oscillations. Such large oscillations represent the Q-switched mode locking (QML) (Figure 2.8). The QML may damage the SESAM. The QML regime is used in applications required very high peak intensity. However, the pulses in this regime typically suffer from poor amplitude stability.

2.3.1 Mode-locking with a saturable absorber

A saturable absorber is an optical material or setup that ensures (or imitates) an absorption, which is reduced with optical intensity. This phenomenon can occur in different media, e.g. dyes, glasses, crystals doped with ions and semiconductors.

The most important properties of saturable absorbers are:

- *modulation depth* is the maximum absorption variation with light intensity,
- *unsaturable losses* is the fraction of the losses which can not be saturated,

- *recovery time* is the decay time of the low-loss state after bleaching by the pulse,
- *saturation intensity* is the optical intensity (power per unit area) it takes in a steady state to reduce the absorption to one half its unbleached value,
- *damage threshold*.

A pictorial schematic that describes the principle of pulse shortening provided by a saturable absorber is presented on Figure 2.9.

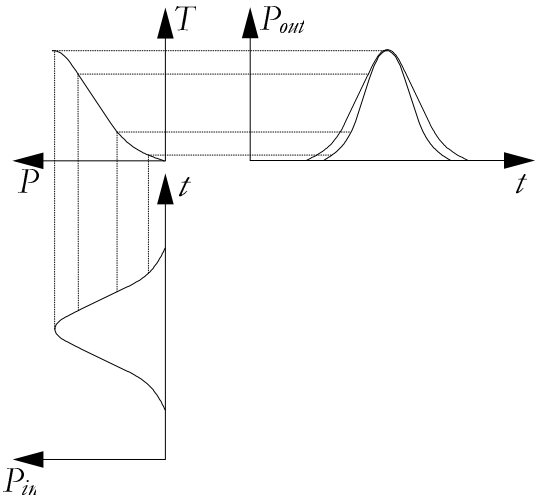

Figure 2.9 – A time-domain graphic representation of the effect of a saturable absorber on pulse shaping.

The top left corner of the Figure 2.9 displays a typical transmission curve of an absorber, which shows that transmission increases as the power of the incident pulse increases. After an incident pulse is coupled to the absorber, it is clear that upon the transmission through the absorber, the low-intensity tails (wings) of the output pulse are attenuated, while the high-intensity center part of the pulse is transmitted without significant loss. As a result, the transmitted pulse has a reduced duration.

When such an absorbing element is used within a laser cavity, it promotes the pulse operation with increased peak power and suppresses the lower-intensity CW light. Because the laser tends to operate with minimum cavity loss per round-trip, the longitudinal modes of the lasers become phase-locked, corresponding in time domain to high intensity short optical pulses.

The pulse shaping process in mode-locked lasers can be described by the equation derived by Haus [23]:

$$T_R \frac{\partial}{\partial T} A(T,t) = \left[g - l + \frac{4g}{\Delta\omega_g^{\,2}} \frac{\partial^2}{\partial t^2} + iD \frac{\partial^2}{\partial t^2} + i\delta \left| A(T,t) \right|^2 + q(T,t) \right] A(T,t), \qquad (2.14)$$

where $\mathcal{A}(T,t)$ is a slowly-varying pulse envelope considered at two time scales, T is of the order of the cavity round-trip time, and t is of the order of the pulse duration. T_R is the cavity round-trip time, g is the saturated gain and l is the loss per cavity round-trip. The third term on the right side of expression (2.14) represents a contribution from a finite gain bandwidth with total homogenous bandwidth $\Delta\omega_g$. D represents the contribution from the GVD, and the term δ represents the self-phase modulation, (SPM). Finally, the term $q(T,t)$ represents the contribution from the saturable absorber. This procedure assumes that the gain and the dispersion are uniformly distributed in the cavity and that the pulse shaping (perturbation) per round-trip is small.

Expression (2.14) is usually studied for three different models of passive mode-locking, represented on Figure 2.10:

(a) a fast saturable absorber,
(b) a slow saturable absorber and gain saturation, and
(c) a slow saturable absorber in the presence of negative dispersion and nonlinearity.

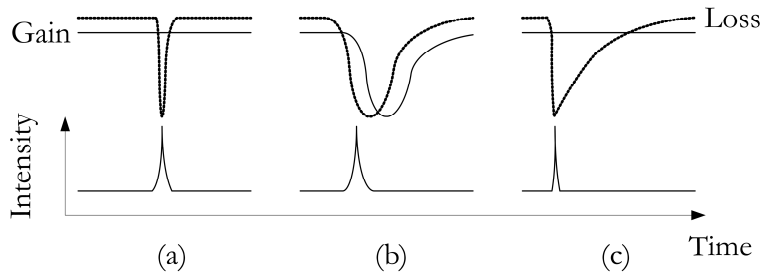

Figure 2.10 – Three models of passive mode-locking: a) fast saturable absorber, b) slow saturable absorber and c) slow saturable absorber and shaping assisted by anomalous dispersion and nonlinearity.

It can be shown that with a fast saturable absorber (model (a)), which responds to the instantaneous intensity changes, and neglecting dispersion and nonlinear effects, the solution for equation (2.14) takes the form of

$$\mathcal{A}_0(t) = \mathcal{A}_0 \operatorname{sech}(t/\tau), \tag{2.15}$$

where τ is given by

$$\tau^2 = \frac{8 g I_{sat} S_{eff,\mathcal{A}}}{q_0 \mathcal{A}_0^{\,2} \Delta\omega_g^{\,2}}, \tag{2.16}$$

Here q_0 represents the saturable absorption, I_{sat} is the saturation intensity and $S_{eff,A}$ is the effective area of the saturable absorber.

For a slow absorber (model (b)), the saturation should be described through the expression

$$q(T,t) = q_i \exp\left[-\int_0^t \left| \mathcal{A}(T,t) \right|^2 / E_A \, dt \right], \tag{2.17}$$

where E_A is the saturation energy of the absorber and q_i represents the losses of the absorber before the pulse arrives. The gain is assumed to saturate in the same manner as an absorber. Therefore,

$$\mathrm{g}(T,t) = \mathrm{g}_i \exp\left[-\int_0^t \left| \mathcal{A}(T,t) \right|^2 / E_\mathrm{g} \, dt \right], \tag{2.18}$$

where g_i is the (unsaturated) gain before the pulse enters the gain medium, and E_g is the gain saturation energy. Assuming that the bandwidth of the gain medium (g(*T*, *t*) is now time dependent!) can be represented by a filter of fixed bandwidth $\Delta\omega_f$, the solution takes a form similar to (2.15), where the parameter τ could be found now from equation

$$\frac{1}{\tau^4} = \frac{\Delta\omega_f^{\,2} \mathcal{A}_0^{\,4}}{16} \left(\frac{q_i}{E_A^{\,2}} - \frac{\mathrm{g}_i}{E_\mathrm{g}^{\,2}} \right). \tag{2.19}$$

Equation (2.19) shows that even with a slow absorber, one can get short pulses without the help of dispersion or non-linear effects, as long as the gain is saturated quickly. Finally, in the third regime (model (c)) presented in Figure 2.10, dispersion and self-phase modulation effects are included. It can be shown that the solutions are of the general type

$$\mathcal{A}(T,t) = \mathcal{A}_0 \left[\mathrm{sech}\left(\frac{t}{\tau} \right) \right]^{(1+j\beta)}, \tag{2.20}$$

where β represents the *chirp* of the pulses. Basically, the pulses can be obtained at both dispersion regimes – anomalous and normal – although the anomalous regime enhances the pulse shortening.

2.4 Semiconductor saturable absorber mirrors

Semiconductor saturable absorber mirrors (SESAMs) have played an increasing role in the field of ultra-short pulse generation [24]. The SESAM uses a saturable absorber in a form of reflector, thus facilitating its integration into laser cavities as a cavity end mirror. A mode-locking technique, which relies upon the use of the nonlinear reflectivity of a SESAM, eliminates the need for critical cavity alignment so that the mirror can be designed to operate in a wide spectral range, and can have relatively large nonlinear reflectivity changes. Ultrashort optical pulses have been produced with this technique using different semiconductor structures and mirror designs.

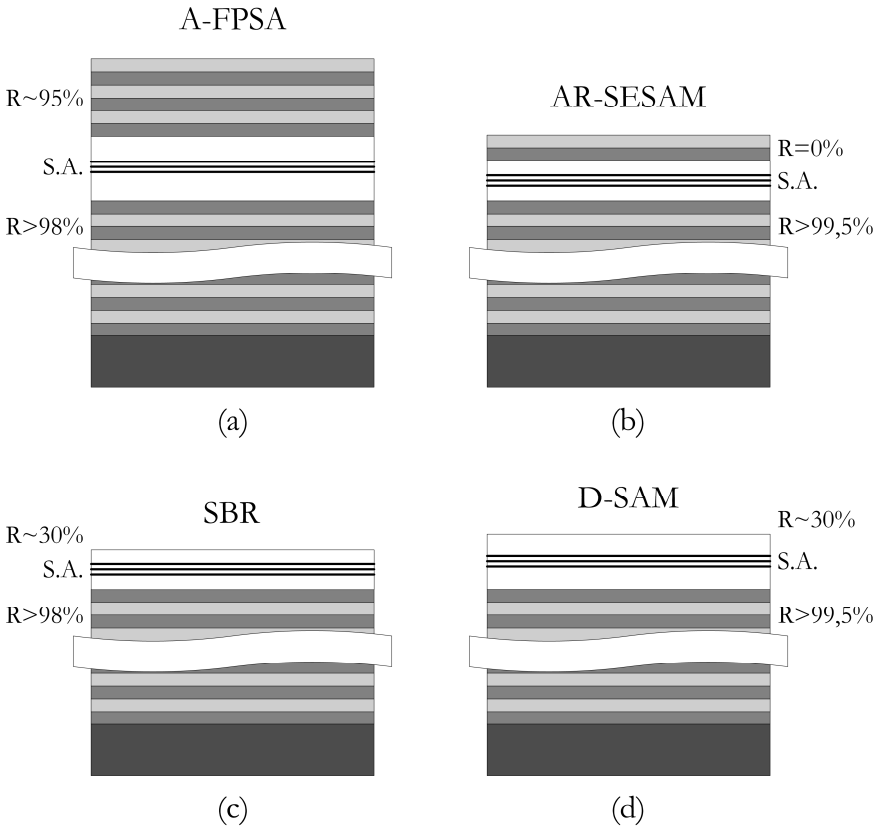

Figure 2.11 – Four main types of SESAM.

The four main categories of SESAM's developed hitherto are illustrated in Figure 2.11. The first structure (a), known as an antiresonant Fabry-Pérot saturable absorber (A-FPSA) was proposed in 1992 [25]. Here, the saturable absorber region is sandwiched between two highly reflective mirrors forming a Fabry-Pérot cavity. The length of this cavity is designed so that the device works out of resonance. A second class of devices (b), the anti-reflection-coated SESAM (AR-SESAM) demonstrated in 1995, uses anti-reflecting coating to eliminate the Fabry-Pérot cavity effects [26]. The third category of the saturable absorbers (c), the saturable Bragg reflector (SBR), was first demonstrated in 1995 [27]. In these devices the saturable absorber is integrated within the last quarter-wavelength pair of the distributed Bragg reflector. Finally, the last category of SESAM (d), a so-called dispersive saturable absorber mirror (D-SAM), is made to operate near the resonance of SESAM microcavity [28]. D-SAM, first demonstrated in 1996, acts simultaneously as a saturable absorber and dispersion compensator. Similar to GTI discussed above, it can generate anomalous dispersion.

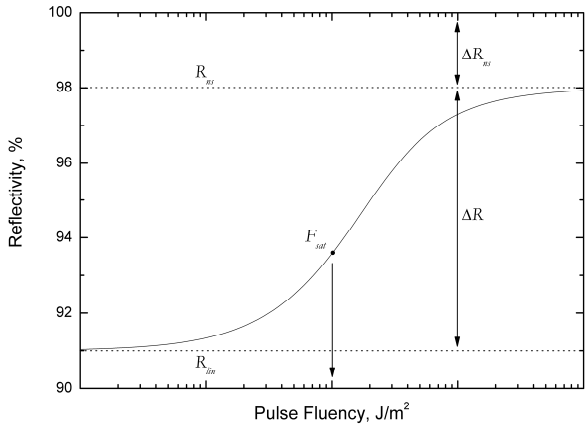

Figure 2.12 – Typical reflectivity curve of a SESAM.

Figure 2.12 shows a typical reflectivity curve of a SESAM. The parameters of a SESAM, the saturation fluency F_{sat}, the modulation depth ΔR, and the non-saturable losses ΔR_{ns} are displayed in the Figure. The nonlinear response of the SESAM can be modeled using the expression [29]

$$R(F) = 1 - R_{ns} - \Delta R \left[\frac{1 - \exp\left(-F/F_{sat}\right)}{F/F_{sat}} \right]. \qquad (2.21)$$

For efficient and self-starting mode-locking, a recovery time of absorption in the range from few picoseconds to tens of ps depending on gain medium and laser cavity is desirable. The recovery time for typical compound semiconductors, in particular multiple-quantum-well structures, is typically about a nanosecond [30]. Therefore, SESAMs fabrication requires special measures to reduce the recovery time. The most used methods for reducing the absorption recovery time are low-temperature growth [31] and heavy ion irradiation [32]. Each of these techniques brings in certain constrains related to fabrication cost, device reliability, degradation of nonlinearity and increased non-saturable losses. In this work we have used ion-implantation to produce crystalline defects and we have exploited the non-radiative recombination centers always introduced by growth of GaInNAs [33, 34].

In terms of the modulation depth required to ensure stable, self-starting, mode-locking of fiber lasers, usually, a modulation of only a few percent is necessary. For solid state lasers this modulation has to be higher, in order to circumvent the higher losses, usually present in solid state cavities.

The presence of a Fabry-Pérot cavity, in most of the SESAMs, can also be exploited to adjust the effective saturation fluency of the devices. This is particularly the case when butt-coupling is to be employed in fiber lasers, because in such devices there is no longer the ability to fine tune the fluency of the pulses, through focusing.

3 Results

This chapter presents experimental results concerning passively mode-locked Yb-doped fiber lasers. The results are grouped in sections describing the performance of SESAMs operating at 1 µm, tunable operation of the mode-locked laser, power scaling using a fiber power amplifier, studies related to the pulse duration, dispersion compensation with a GTI and, finally, pulse generation in a fiber cavity with normal dispersion regime.

3.1 SESAM structure and technology

The saturable absorber mirrors were fabricated by solid-source molecular beam epitaxy (MBE) and were implemented on two material systems – GaInAs and GaInNAs. GaInAs has been normally used for the 0.7–1.2 µm spectral range, while GaInNAs (dilute nitride) has recently been proposed as an alternative to InP-based compounds for the wavelengths above 1.3 µm. The use of GaInNAs at 1 µm was aimed to demonstrate that GaAs-based quantum wells can be employed in an extended wavelength range from 1 to 1.5 µm [35] and that dilute nitride absorbers are faster than GaInAs based absorbers.

Figure 3.1 shows a low-intensity reflectivity spectrum of the GaInNAs SESAM. This component is a SBR type mirror, discussed in section 2.4, with the usable wavelength range ranged from 950 to 1050 nm. The dip in the centre is caused by the absorption of five GaInNAs quantum wells (QWs) located on top of the DBR composed of 26 pairs of AlAs/GaAs quarter-wavelength layers. No post-growth treatments were applied to the structure prior to measuring the reflectivity.

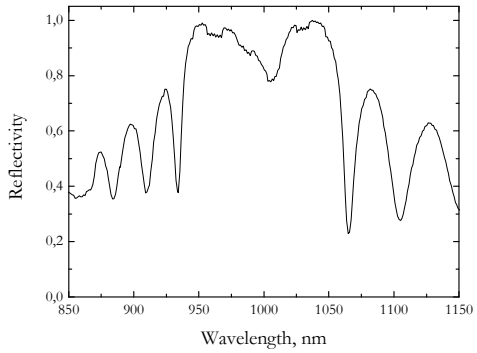

Figure 3.1 – Reflectivity spectrum of a GaInNAs absorber.

The nonlinear reflectivity response of this device shows a high modulation depth of 12 % in Fig. 3.2. The modulation depth was intentionally increased since it was

demonstrated, that a large nonlinear response in the SESAM reflectivity improves the starting capability of the passive mode-locking in fiber lasers [36]. A high value of ΔR, however, may provoke the low-frequency Q-switched instabilities. The saturation fluency of this device was 3 $\mu J/cm^2$.

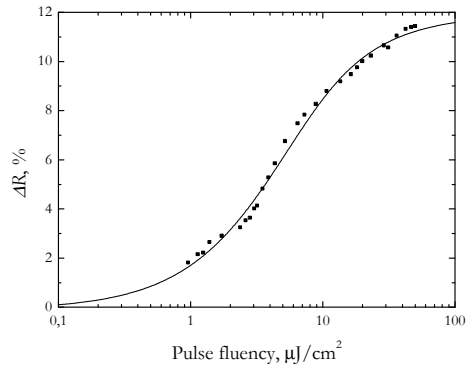

Figure 3.2 – Nonlinear reflectivity of a GaInNAs absorber mirror as a function of pulse fluency.

The "reference" absorber based on GaInAs material uses an AlAs/GaAs DBR with 25 pairs of $\lambda/4$ layers. The active region includes two GaInAs QWs. The central wavelength of the DBR stop-band was shifted to the longer wavelengths compared to the GaInNAs absorber, as shown on Figure 3.3. The combined operation range of the two absorbers thus covers the entire gain bandwidth of ytterbium fiber from 977 to 1150 nm. In order to reduce the absorption recovery time, this absorber was irradiated with 10-MeV Nickel ions with a dose of 10^{12} ions/cm^2 after epitaxial growth.

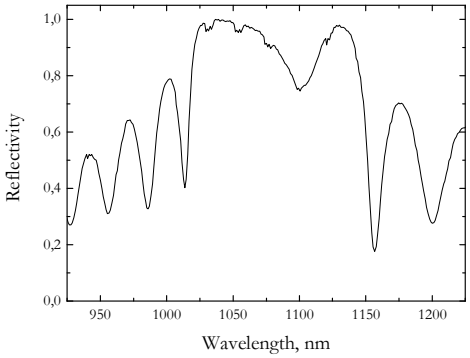

Figure 3.3 – Reflectivity spectrum of a GaInAs absorber.

3.2 Tunable mode-locked-laser

The laser with a linear cavity, shown in Figure 3.4, incorporates a pair of 1600 lines/mm diffraction gratings (DG) for dispersion compensation [Paper III]. Since the reflectivity of gratings is polarization dependent, the polarization controller (PC) was included, in order to minimize the losses in the DG. The cavity was

terminated by a SESAM and by a loop mirror (LM) acting also as an output coupler. LM has the reflectivity of ~55–60 % in the wavelength range from 980 to 1100 nm.

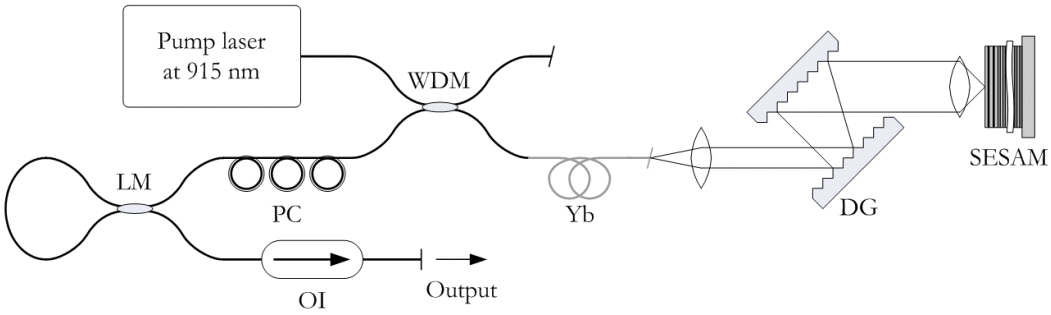

Figure 3.4 – Laser setup with a grating pair used for dispersion compensation and wavelength tuning.

The Yb-doped fiber used in this experiment had a core diameter of 6.3 μm, a NA of 0.13 and a cut-off wavelength of 920 nm. Gain fiber absorption was ~434 dB/m at 976 nm, while at 915 nm it was estimated to be ~140 dB/m. This fiber was core-pumped through a wavelength division multiplexer (WDM) by a 100 mW pump laser diode emitting at 915 nm.

With a proper alignment, stable mode-locking was obtained with an average output power of 15 mW measured after the optical isolator (OI). This isolator with 3-dB loss was used to protect the cavity against instabilities that may arise from spurious reflections.

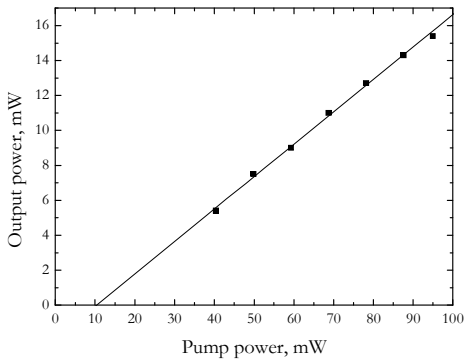

Figure 3.5 – Output power of the mode-locked pulses.

With a 35 cm long Yb-doped fiber and a 915/990 nm WDM coupler, the spectrum of mode-locked pulses was centered at 980 nm. The pulse duration was 2.47 ps. The corresponding time-bandwidth product (TBP) was 0.56. The large value of TBP (1.75 times the transform limited value) was mainly due to the pulse broadening in the fiber pigtailed optical isolator. This issue will be further discussed in Section 3.4.

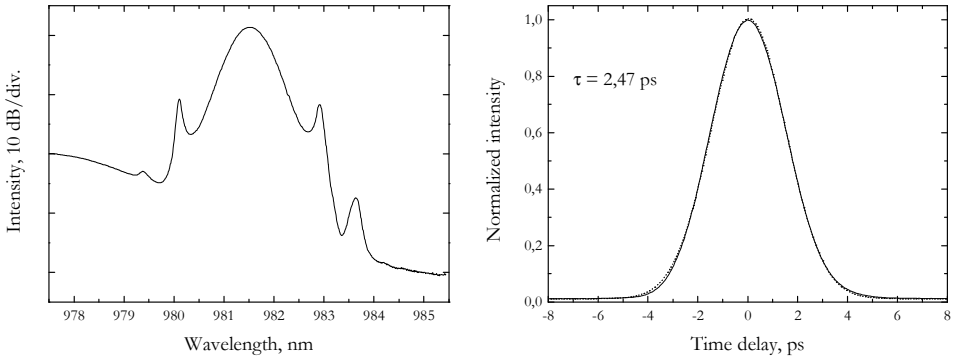

Figure 3.6 – Spectrum and autocorrelation of the pulses around 980 nm.

The wavelength tunability in this laser was performed using two setups. First, a coarse wavelength range selection was made by tilting the second diffraction grating of the compensator pair. This tilting allowed for wavelength-selective feedback to be achieved from an angularly dispersed radiation, as shown in Figure 3.7 (a). A fine tuning was accomplished by lateral shifting of the objective used to focus the light onto the absorber, as shown in Figure 3.7 (b). The fine tuning was precisely controlled by a micro-positioning stage translating the focusing objective.

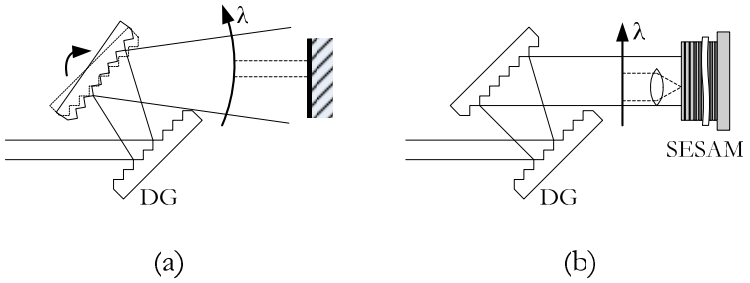

Figure 3.7 – The two tuning methods.

Combining these two methods, tuning of the mode-locked pulses from 977 to 1020 nm was demonstrated, as shown in Figure 3.8. The intensity of the spectra was normalized, although optical power was approximately the same in the entire wavelength range.

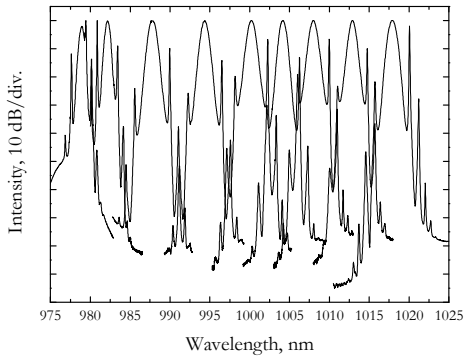

Figure 3.8 – Examples of pulses in the 980 to 1020 nm tuning range.

For fibers longer than 40 cm, the laser tended to operate at ~1030 nm since 980 nm radiation is efficiently reabsorbed in the ytterbium fiber. It should be noted that unlike

cladding pumped Yb-doped fiber lasers operating at 980 nm, where unwanted gain at 1040 nm causes significant problems [4], in core-pumped lasers 980 nm lasing can be achieved relatively easy as long as pump power is high enough to create population inversion at far (from the pumping source) end of the doped fiber. Therefore, to achieve a long-wavelength operation, the length of the doped fiber was then increased to 50 cm. To avoid cavity loss at longer wavelengths due to signal leakage through a WDM, the latter was replaced with a 915/1050 nm WDM optimized for operation at 1.05 µm. Because the DBR used in GaInNAs absorber limits the tuning to the longer wavelength to 1040 nm, as seen from Figure 3.1, the DBR mirror was replaced with the GaInAs device described above.

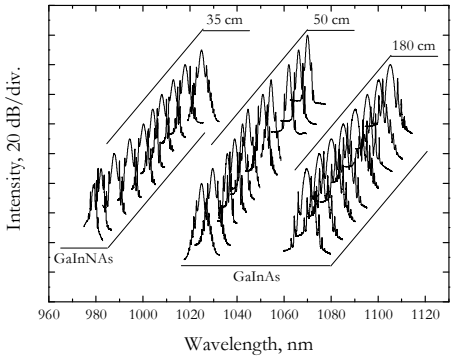

Figure 3.9 – Full tuning range of the laser

Figure 3.9 illustrates three tuning bands, which have a large combined bandwidth from 977 to 1115 nm. The laser with tuning in the 1070–1117 nm band uses the length of doped fiber of 180 cm and a 915/1090 nm WDM together with GaInAs absorber.

3.3 Power scaling

To increase the pulse energy, a MOPA setup was implemented using a double clad fiber power amplifier provided by Fianium Ltd. The gain section of the amplifier was composed of Yb double-clad fiber that uses end-coupling technique with the broad-area 915 nm laser diodes. The scheme used to amplify the pulses is presented on Figure 3.10. Before the amplifier, a 5%-tap coupler and a 915/990 nm WDM were added. These ensure master laser control and provided laser protection against back-scattered emission from the high-power amplifier.

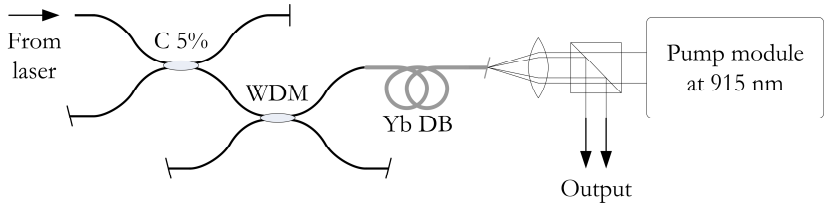

Figure 3.10 – Amplifier setup.

The pump module combined the output of four laser diodes and was able to produce up to 4 W of power at 915 nm. The double-clad gain fiber with a length of 50 cm had a pump-cladding diameter of 50 μm. Figure 3.11 shows two spectra of the amplifier output, one without the input signal and another with the input signal launched from the master laser. Fig. 3.11 confirms an efficient gain saturation of the amplifier. Therefore, reasonable energy extraction is expected with our master oscillator served as a seed source for the power amplifier.

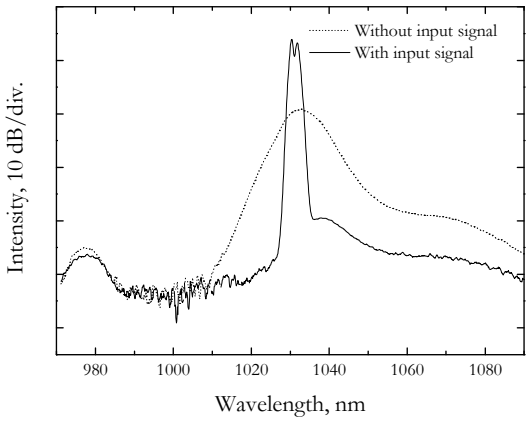

Figure 3.11 – Output spectra of the amplifier with and without an input signal from the master oscillator.

The laser used in this experiment incorporates 50-cm-long Yb-doped fiber and the GaInAs absorber. The laser operating wavelength could be tuned to the peak of the amplified spontaneous emission (ASE) of the amplifier corresponding to the gain spectral maximum, as seen from Figure 3.11. With 15 mW of laser power, the amplifier was able to produce pulses with ~700 mW of average power at pump power of 3.5 W. Figure 3.12 shows no saturation in the output power. Higher output powers would be possible with appropriate pump sources and proper cooling, possibly water cooling system.

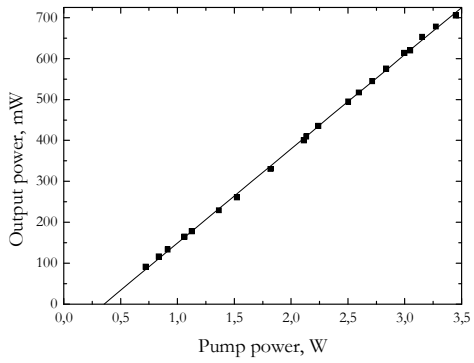

Figure 3.12 – Output power after amplification.

The pulse duration from the master laser was 3 ps. No significant temporal degradation was observed after a short-length fiber power amplifier. The repetition rate corresponding to the cavity roundtrip time was about 33 MHz that resulted in the pulse energy of 23 nJ and a peak power of 6 kW.

3.4 Optimization of the pulse duration

The master source used in our power scaling experiments was further optimized to achieve ultrashort pulses. First, we have studied the spectral dependence of the pulse duration for different values of dispersion created by the grating compensator. The results of these measurements are presented in Figure 3.13. For a specific compensator parameter and doped fiber length, the pulse duration increased linearly with the wavelength, as seen in Fig 3.13.

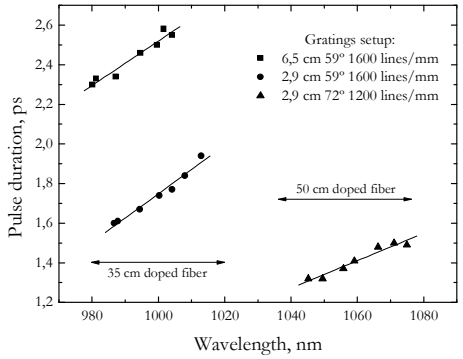

Figure 3.13 – Pulse duration as function of wavelength and dispersion.

The increase of the pulse duration can be explained assuming that the grating pair over-compensated the dispersion introduced by the fiber. With the increase of the wavelength, the dispersion generated by the grating pair increases too, leading to the increase of overall (anomalous) dispersion of the laser cavity and, hence, resulting in longer pulses.

This explanation could be further supported by measuring the pulse duration for different grating separations. Figure 3.14 displays pulse duration versus pump power as the grating separation as a parameter. The laser wavelength was fixed at 1040 nm.

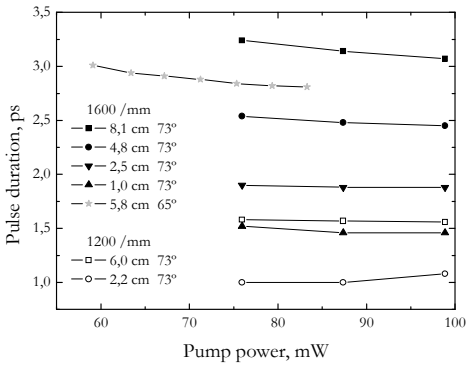

Figure 3.14 – Pulse duration versus pump power for different dispersions of the grating-pair compensator.

We can see that the pulse duration decreases with the decrease of the grating separation and, hence, the decrease of the anomalous dispersion of the laser cavity.

Finally, the external pulse compression at the output of the laser was studied, using an additional grating pair. Figure 3.15 shows a plot of the pulse duration as a function of the gratings' separation in the external compressor.

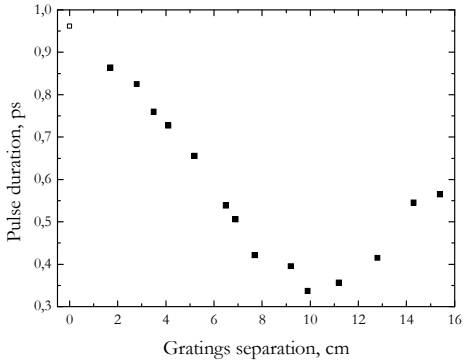

Figure 3.15 – Pulse duration as function of the gratings separation.

It should be mentioned that the results presented in Figure 3.15 were corrected for the pulse broadening introduced by the pigtails of an optical isolator located at the output of the laser. Conversion was performed by adding the fibers with different lengths consecutively to the output of the laser, and then the duration of the pulse before the optical isolator was found by the extrapolation to the zero-length fiber (this point is show as a hollow square for the 0 cm grating separation). The minimum pulse duration thus obtained was 340 fs corresponding to a TBP of 0.57. It should be mentioned that if the pulse width is not corrected, then the minimum pulse width obtained, after the grating pair, was just under 1 ps.

3.5 Dispersion compensation with GTI

The demonstration of a GTI as a dispersion compensator in a fiber laser was the next challenge. In order to minimize the dispersion of the fiber section of the cavity, a fiber with an extremely high concentration of Yb-ions was used. These fibers were developed by Liekki, and despite their high doping level, the fibers do not suffer significantly from the presence of ion clusters owing to Liekki's direct nanoparticle deposition technique [37], [38].

The numerical aperture of the fiber is 0.22 and the cut-off wavelength was 910 nm. The fiber absorption at 976 nm was over 1900 dB/m and at 915 nm the absorption was estimated to be of 500 dB/m. These values allow for reduction of the fiber length used in a laser cavity down to a few centimeters.

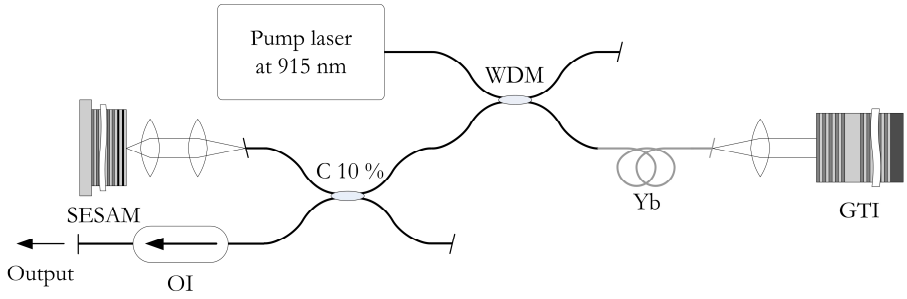

Figure 3.16 – Laser setup using a GTI compressor.

The setup that was used to demonstrate the dispersion compensation with a GTI is shown in Figure 3.16 [Paper IV]. The linear cavity was terminated on one end by the GaInNAs absorber described above, and by the GTI on the other end. A 10 % output coupler was introduced in the cavity to facilitate the extraction of the laser signal. The length of Yb-doped fiber used as a gain medium was only 2.5 cm. The total length of the fiber in the laser cavity including the passive components (WDM and an output coupler) was 74 cm giving the total normal dispersion of +0.04 ps^2.

The dielectric GTI was built using an electron-beam evaporator and consisted of a bottom DBR with 10 pairs of alternate layers of TiO_2 / SiO_2, a buffer layer with 0.7 μm of SiO_2 and a top mirror with 4.5 pairs of TiO_2 / SiO_2. The length of the cavity was designed so that the cavity resonance was positioned in the 1020–1030 nm range.

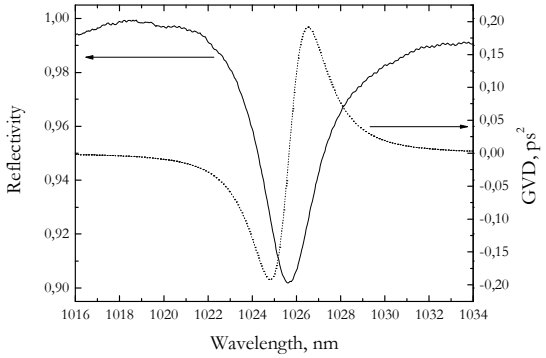

Figure 3.17 – Measured reflectivity and calculated dispersion of the dielectric GTI.

The reflectivity spectrum of the GTI sample, shown in Figure 3.17, has the cavity resonance at 1026 nm. The calculated dispersion, shown with a dashed line, indicates that this reflector is able to introduce up to –0.20 ps^2 of anomalous dispersion at particular wavelength. It should be noted that to generate such a high value of anomalous dispersion, the device needs to be operated at the resonance. Although, the experimental sample used in this study has a loss of 9 % near the resonant wavelength, this loss could be avoided with the improvements in the material quality and evaporation technique.

Without optical filtering used in the laser cavity, the operation wavelength of this fiber laser is determined by the interplay between few effects: the dispersion of the GTI reflector and the reflectivities of the GTI and SESAM.

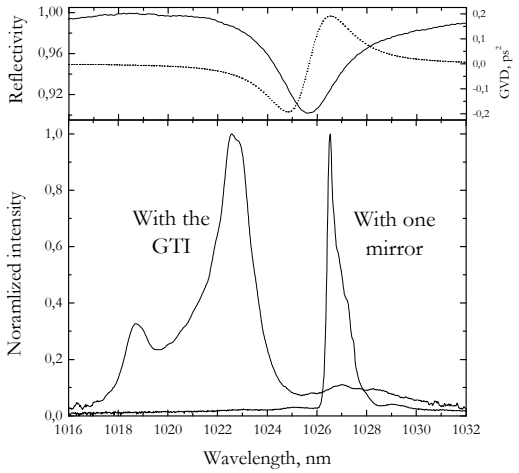

Figure 3.18 – Spectra of the pulses with an ordinary high-reflective mirror and with the GTI.

Figure 3.18 shows the laser spectra with and without dispersion compensation performed using the GTI. With the GTI placed into the cavity, the SESAM-supported mode-locked operation self-starts at 1023 nm. At this wavelength, the GTI generates an anomalous dispersion of –0.05 ps^2 and introduces a loss of ~1 %. Pulse operation at the longer wavelength of 1025 nm with a larger anomalous dispersion could not be achieved because of higher loss that prevented reliable pulse operation. The low value of anomalous dispersion induced by the GTI was, however, sufficient to compensate the dispersion in the cavity with the short length of the fiber. The estimation shows that the laser was operating in the anomalous dispersion regime.

When the GTI was replaced with a high-reflective mirror, mode-locked operation could still be achieved due to the action of the high-modulation depth SESAM, as discussed above. However, the pulse width increased significantly and the bandwidth of the optical spectrum decreased accordingly, as seen from Figure 3.18. The central pulse wavelength was shifted to longer wavelengths closer to the gain maximum of the ytterbium fiber.

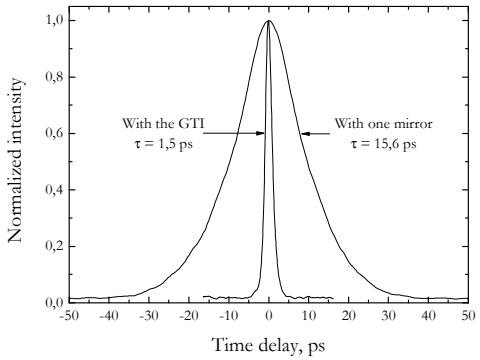

Figure 3.19 – Pulse duration with one mirror and with the GTI.

The GTI resulted in a dramatic pulse shortening, as illustrated in Figure 3.19. The pulse compression by a factor of 10 was achieved owing to the dispersion compensation induced by the GTI.

3.6 Stretched-pulse laser

Finally, the generation of mode-locked pulses in a cavity without any dispersion compensation was explored. To decrease the cavity length, and therefore, the total fiber dispersion further, an active fiber was placed in a loop mirror served as a cavity mirror, as shown in Figure 3.20 [Paper VI]. The other mirror was formed by the GaInNAs absorber described above.

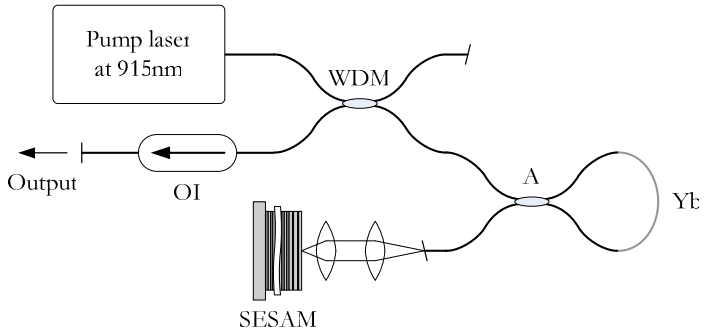

Figure 3.20 – Stretched pulse fiber laser.

The coupler (A) had a wavelength-dependent splitting ratio. The coupler ensured the operation of the loop mirror with reflectivity of 80 % at 1020 nm. At the pump wavelength of 915 nm, the coupler acted as a symmetrical beam splitter. This allows to pump the gain fiber located in the loop uniformly thus providing nearly constant inversion along entire piece of highly-doped fiber. The Yb fiber was identical to the fiber used in Section 3.5.

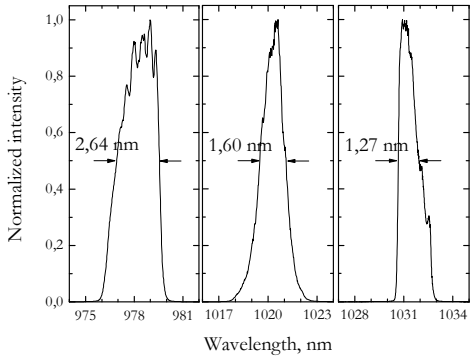

Figure 3.21 – Spectra of the pulses obtained by using 2.1 cm (left), 3.4 cm (middle) and 4.1 cm (right) of ytterbium doped fiber.

Figure 3.21 shows the spectra obtained with three different lengths of doped fiber. As can be seen, the length of an active fiber determines the wavelength of the pulses. This feature is due to the strong re-absorption of the radiation in the long fiber, which

is then re-emitted at longer wavelengths. The re-absorption obviously increases with the length of the ytterbium doped fiber.

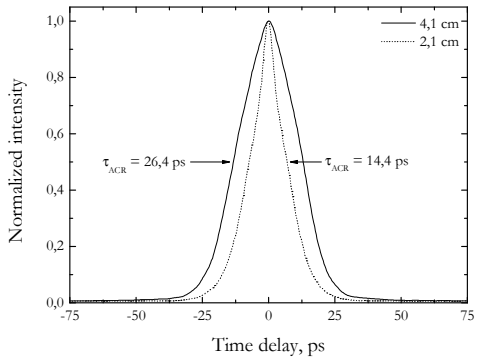

Figure 3.22 – Autocorrelation traces of the pulses obtained with 2.1 and 4.1 cm of Yb-doped fiber.

The autocorrelation traces for passive mode-locked operation with the length of active fiber of 2.1 and 4.1 cm are shown in Figure 3.22. Because of the stretched-pulse regime, the pulse shapes could be fitted with neither Gaussian nor $sech^2$ functions. Figure shows the FWHM of the autocorrelation traces.

4 Conclusions

The main scope of this thesis is a comprehensive study of the SESAM technology for the passive mode-locking of Yb-doped fiber lasers operating at 1 μm wavelength range. The results obtained in the research include the utilization of GaInNAs composition as a fast saturable absorber material for ytterbium systems, the use of Gires–Tournois interferometers for dispersion compensation in a short-length fiber cavity, the demonstration of a tunable mode-locked laser with the tuning range over 140 nm, and a study of stretched-pulse lasers with large normal cavity dispersion.

The results demonstrate that using semiconductor saturable absorber mirrors makes it possible to reliably mode-lock fiber lasers with different values of cavity dispersion in a broad spectrum ranged from 900 to 1100 nm. We have discussed basic properties, technical challenges and methods to achieve high average and peak powers from all-fiber devices. We have also presented results on the development of compact picosecond laser sources capable of delivering pulses with energy of 23 nJ at the repetition rate of 30 MHz.

We believe that further progress in the ultrafast fiber systems is expected, following the advances in the fiber technology. Improving the output power through the optimization of the doped fiber, using photonic crystal fibers for controlling the nonlinear effects and for dispersion compensation would result in high-power and compact all-fiber ultrafast systems of high commercial value.

References

1 Michael A. Marcus, “Fiber Optic Technology and Applications”, Vol. 386, 1999.

2 M.J.F. Digonnet (Editor), “Rare earth doped fiber lasers and amplifiers”, Marcel Dekker, New York, ISBN 0-8247-8785-4, 1993.

3 J. Swiderski, A. Zajac, M. Skorczakowski, Z. Jankiewicz and P. Konieczny, “Rare earth doped high power fiber lasers generating in near infrared range”, Opto-Electronics Review, vol. 12, pp. 169–173, April 2004.

4 K. H. Ylä-Jarkko, R. Selvas, D. B. S. Soh, J. K. Sahu, C. A. Codemard, J. Nilsson, S. A. Alam and A. B. Grudinin, “A 3.5W 977 nm cladding-pumped jacketed-air clad ytterbium-doped fiber laser”, Proc. Advanced Solid-State Photonics, postdeadline PDP2, San Antonio, Texas, February 2003.

5 G.P. Agrawal, “Nonlinear fiber optics”, 2nd Edition, Academic Press, California, ISBN 0-12-045142-5, 1995.

6 G. Keiser, “Optical fiber communications”, 2nd Edition, McGraw Hill, ISBN 0-07100785-7, 1991.

7 S. Gray and A. B. Grudinin, “Soliton fiber laser with a hybrid saturable absorber”, Optics Letters, vol. 21, No. 3, 1996.

8 J.C. Knight, J. Arriaga, T.A. Birks, A. Ortigosa-Blanch, W. J. Wadsworth and P. St. J. Russell, “Anomalous dispersion in photonic crystal fiber”, IEEE Photon. Tech. Lett., vol. 12, pp. 807–809, April 2000.

9 C.J.S. de Matos, J.R. Taylor, T.P. Hansen, K.P. Hansen and J. Broeng, “All-fiber chirped pulse amplification using highly-dispersive air-core photonic bandgap fiber”, Opt. Express, vol. 11, pp. 2832–2837, October 2003.

10 E.B. Tracy, “Optical pulse compression with diffraction gratings”, IEEE J. Quantum Electron., vol. 5, pp. 454–458, September 1969.

11 F. Gires and P. Tournois, “Interféromètre utilisable pour la compression d’impulsions lumineuses modulées en fréquence,” C. R. Acad. Sci. Paris, vol. 258, pp. 6112–6115, June 1964.

12 J. Heppner and J. Kuhl, “Intracavity chirp compensation in a colliding pulse mode-locked laser using thin-film interferometers”, Applied Phys. Lett. 47, 453–455, 1985.

13 J. Kuhl and J. Heppner, “Compression of femtosecond optical pulses with dielectric multilayer interferometers”, IEEE J. Quantum Electron. Vol. QE-22, issue 1, 182–185, January 1986.

14 A. Isomäki, A. Vainionpää, J. Lyytikäinen and O. G. Okhotnikov, “Semiconductor mirror for dynamic dispersion compensation”, Appl. Phys. Lett., 82, pp. 2773–2774, 2003.

15 U. Keller, K.J. Weingarten, F.X. Kärtner, D. Kopf, B. Braun, I.D. Jung, R. Fluck, C. Hönninger, N. Matuschek and J.A. Aus, “Semiconductor saturable absorber mirrors (SESAM’s) for femtosecond to nanosecond pulse generation in solid-state lasers”, IEEE J. Sel. Topics in Quantum Electronics, vol. 2, pp. 435–453, September 1996.

16 G. J. Spühler, R. Paschotta, R. Fluck, B. Braun, M. Moser, G. Zhang, E. Gini and U. Keller, “Experimentally confirmed design guidelines for passively Q-switched microchip lasers using semiconductor saturable absorbers”, J. Opt. Soc. Am. B 16(3), 376–387, 1999.

17 A.E. Siegman, “Lasers”, University Science Books, California, ISBN 0-935702-11-5, 1986.

18 D. H. Sutter, G. Steinmeyer, L. Gallmann, N. Matuschek, F. Morier-Genoud, U. Keller, V. Scheuer, G. Angelow and T. Tschudi, “Semiconductor saturable-absorber mirror-assisted Kerr-lens mode-locked Ti:sapphire laser producing pulses in the two-cycle regime”, Opt. Lett. 24, 631–633, 1999.

19 O. Okhotnikov, A. Grudinin and M. Pessa, “Ultra-fast fibre laser systems based on SESAM technology: new horizons and applications”, New J. Phys., vol. 6, 177, November 2004.

20 Matei Rusu, Robert Herda and Oleg G. Okhotnikov, “Passively synchronized Erbium (1550 nm) and Ytterbium (1040 nm) mode-locked fiber lasers sharing the cavity”, Opt. Lett., 29, pp. 2246–2248, 2004.

21 Matei Rusu, Robert Herda and Oleg G. Okhotnikov, “Passively synchronized two-color mode-locked fiber system based on master-slave lasers geometry”, Opt. Express, 12, pp. 4719–4724, 2004.

22 Matei Rusu, Robert Herda and Oleg G. Okhotnikov, “1.05-µm mode-locked Ytterbium fiber laser stabilized with the pulse train from a 1.54-µm laser diode”, Opt. Express, 12, pp. 5258–5262, 2004.

23 H.A. Haus, “Mode-locking of lasers”, IEEE J. Sel. Topics on Quantum Electron., vol. 6, pp. 1173–1185, November/December 2000.

24 U. Keller, K. J. Weingarten, F. X. Kärtner, D. Kopf, B. Braun, I. D. Jung, R. Fluck, C. Hönninger, N. Matuschek and J. Aus der Au, IEEE J. Sel. Top. Quantum Electron. 2, 435, 1996.

25 U. Keller, D.A.B. Miller, G.D. Boyd, T.H. Chiu, J.F. Fergunson and M.T. Asom, “Solid state low loss intracavity saturable absorber for Nd:YLF lasers: an antiressonant semiconductor Fabry-Pérot saturable absorber”, Opt. Lett., vol.17, pp. 505–507, April 1992.

26 L.R. Brovelli, I.D. Jung, D. Kopf, M. Kamp, M. Moser, F.X. Kärtner and U. Keller, “Self-starting soliton mode-locked Ti:Sapphire laser using a thin semiconductor saturable absorber”, IEEE Electron. Lett., vol. 31, pp. 287–289, February 1995.

27 S. Tsuda, W.H. Knox, E.A. Souza, W.Y. Jan and J.E. Cunningham, “Low-loss intracavity AlAs/GaAs saturable Bragg reflector for femtosecond mode-locking in solid state lasers”, Opt. Lett., vol. 20, pp. 1406-1408, July 1995.

28 D. Kopf, G. Zhang, R. Fluck, M. Moser and U. Keller, “All-in-one dispersion-compensating saturable absorber mirror for compact femtosecond laser sources”, Opt. Lett., vol. 21, pp. 486–288, April 1996.

29 M. Haiml, R. Grange and U. Keller, “Optical characterization of semiconductor saturable absorbers”, Appl. Physics B, vol. 79, pp. 331–339, August 2004.

30 S. Gray and A. B. Grudinin, “Soliton fiber laser with a hybrid saturable absorber”, Opt. Lett., vol. 21, 3, pp. 207–209, 1996.

31 Shantanu Gupta, John F. Whitaker and Gerard A. Mourou, “Ultrafast carrier dynamics in III-V semiconductors grown by molecular-beam epitaxy at very low substrate temperatures”, IEEE J. of Quantum Electronics, vol. 28, issue 10, pp. 2464–2472, October 1992.

32 E. Lugagne Delpon, J. L. Oudar, N. Bouché, R. Raj, A. Shen, N. Stelmakh and J. M. Lourtioz, “Ultrafast excitonic saturable absorption in ion-implanted InGaAs/InAlAs multiple quantum wells” Appl. Phys. Lett., vol. 72, pp. 759–761, 1998.

33 V. D. S. Dhaka, N. V. Tkachenko, E.-M. Pavelescu, H. Lemmetyinen, T. Hakkarainen, M. Guina, J. Konttinen, O. Okhotnikov, M. Pessa, K. Arstila and J. Keinonen, ”Ni^{+}-irradiated InGaAs/GaAs quantum-wells: picosecond carrier dynamics”, New J. Phys., 7, 2005.

34 A. Härkonen, T. Jouhti, N. V. Tkachenko, H. Lemmetyinen, B. Ryvkin, O.G. Okhotnikov, T. Sajavaara and J. Keinonen, “Dynamics of photoluminescence in GaInNAs saturable absorber mirrors”, Appl. Phys. A., 77, pp. 861–863, 2003.

35 O. G. Okhotnikov, T. Jouhti, J. Konttinen, S. Karirinne and M. Pessa, “1.5-µm monolithic GaInNAs semiconductor saturable absorber mode locking of an erbium fiber laser”, Opt. Lett., 28, pp. 364–366, 2003.

36 Robert Herda and Oleg G. Okhotnikov, “Dispersion compensation-free fiber laser mode-locked and stabilized by high-contrast saturable absorber mirror”, IEEE J. Quantum Electron., vol. QE-40, pp. 893–899, 2004.

37 S. Tammela, P. Kiiveri, S. Sarkilahti, M. Hotoleanu, H. Valkonen, M. Rajala, J. Kurki and K. Janka, “Direct nanoparticle deposition process for manufacturing very short high gain Er-doped silica glass fibers,” in Proceedings of the 28th European Conference on Optical Communication, P. Danielsen, ed. (European Conference on Optical Communication, Lyngby, Denmark, 2002), vol. 4, paper 9.4.2., 2002.

38 S. Tammela, M. Hotoleanu, P. Kiiveri, H. Valkonen, S. Sarkijarvi and K. Janka, ”Very Short Er-Doped Silica Fiber for L-band Amplifiers”, in Proceedings of OFC 2003, vol. 1, paper WK3, 2003.

Appendices

Publication 1.

"Mode-locked ytterbium fiber laser tunable in the 980–1070 nm spectral range", O. G. Okhotnikov, **L. A. Gomes**, N. Xiang, T. Jouhti and A. Grudinin, Optics Letters, vol. 28, pp. 1522–1524, September 2003.

Publication 2.

"980-nm picosecond fiber laser", O. G. Okhotnikov, **L. A. Gomes**, N. Xiang, T. Jouhti, A. K. Chin, R. Singh and A. B. Grudinin, IEEE Photonic Technology Letters, vol. 15, p. 1519–1521, November 2003.

Publication 3.

"Picosecond SESAM-based Ytterbium Mode-Locked Fiber Lasers", **L. A. Gomes**, L. Orsila, T. Jouhti and O. G. Okhotnikov, Journal of Selected Topics on Quantum Electronics, vol. 10, pp. 1902–1906, January/February 2004.

Publication 4.

"Mode-locked ytterbium fiber lasers", L. Orsila, **L. A. Gomes**, N. Xiang, T. Jouhti and O. G. Okhotnikov, Applied Optics, vol. 43, pp. 129–136, March 2004.

Publication 5.

"Mode-locked ytterbium fiber laser tunable in the 980–1070 nm spectral range", **L. A. Gomes**, N. Xiang, T. Jouhti, O. G. Okhotnikov and A. Grudinin, 87th OSA Annual Meeting "Frontiers in Optics", Tucson, Arizona, USA, October 2003.

Publication 6.

"140-MHz stretched pulse ytterbium fiber laser operating in the 980–1030 nm spectral range", **L. A. Gomes**, N. Xiang, T. Jouhti, O. G. Okhotnikov, M. Hotoleanu, A. Salomaa and S. Tammela, 87th OSA Annual Meeting "Frontiers in Optics", Tucson, Arizona, USA, October 2003.

Tampereen teknillinen yliopisto
PL 527
33101 Tampere

Tampere University of Technology
P.O. Box 527
FIN-33101 Tampere, Finland